PHILOSOPHICAL TRANSACTIONS OF THE ROYAL SOCIETY A MATHEMATICAL, PHYSICAL & ENGINEERING SCIENCES

Snapshot Echo-Planar Imaging Methods: Current Trends and Future Perspectives [and Discussion]

P. Mansfield, A. M. Blamire, R. Coxon, P. Gibbs, D. N. Guilfoyle, P. Harvey, M. Symms, J. C. Waterton, P. A. Bottomley, A. N. Garroway and G. K. Radda

Phil. Trans. R. Soc. Lond. A 1990 **333**, 495-506
doi: 10.1098/rsta.1990.0177

Snapshot echo-planar imaging methods: current trends and future perspectives

By P. Mansfield, A. M. Blamire, R. Coxon, P. Gibbs, D. N. Guilfoyle, P. Harvey and M. Symms

Department of Physics, University of Nottingham, University Park, Nottingham NG7 2RD, U.K.

Ultra-high-speed imaging methods have gained in credibility over the past two years by virtue of improvements in imaging quality. This has come about by increases in both signal:noise ratios and image matrix size. Signal:noise improvements have been gained largely by use of higher magnetic field strengths.

In echo-planar imaging (EPI) the image matrix size, and hence pixel resolution, depends on the use of large rapidly switched magnetic field gradients. Improvements in gradient coil design, the introduction of active magnetic screening of the coils and the availability of more powerful amplifiers, have all helped to achieve higher in-plane resolution.

On our home-built system, operating at 0.5 T, the pixel resolution is currently $3 \times 1.5\ \mathrm{mm}^2$ for a slice thickness of *ca.* 10 mm.

The principles of EPI are briefly outlined and results of current techniques presented. Future perspectives will be directed to combinations of EPI with spectroscopy and new developments in echo-volumar imaging.

1. Introduction

Echo-planar imaging (EPI) is an ultrafast high-speed imaging technique which produces snapshot images in times ranging from 32 to 128 ms (Mansfield 1977; Mansfield & Pykett 1978; Mansfield & Morris 1982). The EPI method evolved from the principles of NMR imaging introduced by Mansfield & Grannell in 1973 (1973, 1975). In that work the analogy was drawn between the NMR imaging process and plane-wave scattering in optics. The concept of reciprocal lattice space was introduced into imaging at that point and now forms the basis of description of all NMR imaging techniques. Indeed, the so-called *k*-space trajectory approach to NMR imaging allows comparison between all NMR imaging methods and has led to novel imaging techniques, as well as improvements to a number of existing techniques (Ljunggren 1983; Mansfield 1988).

The speed at which imaging is performed emerged as an important factor for consideration early on in the development of the subject. It was recognized that if NMR imaging were to be clinically useful, it was important to image rapidly. In the body there are typically three important timescales that must be considered if images are not to suffer from motional blurring artefact. These timescales correspond to respiratory motion, peristaltic motion and cardiac motion. Fit persons can be expected to hold their breath for perhaps 30 s, whereas patients often find it difficult to hold their breath for more than about 10 s. This is particularly true of the aged and infirm. Thus to obtain good thoracic images or indeed images of liver and kidneys free from diaphragmatic motion, it is necessary to image in times between

1 and 10 s. For peristaltic motion the timescale is typically *ca.* 5 s. This will depend on intestinal motility and in particular whether the stomach and intestines have been recently stimulated by ingestion of food. The third régime is cardiac motion and here it is necessary to image in times much less than the cardiac cycle itself, i.e. 65 ms or less.

The recent development of other fast imaging techniques such as FLASH and snapshot FLASH (Frahm *et al.* 1986; Haase *et al.* 1989) means that imaging at the 10 s timescale is now also possible by these methods. Snapshot FLASH, for example, is able to produce images at below 1 s, but with consequent loss in signal:noise ratio and contrast.

With EPI the total range of timescales can be tackled successfully. Of course, other parts of the anatomy where speed is not a prerequisite can be studied as well, for example, the pelvis and the head. Indeed, as we shall see, it is possible by EPI to study regions of the anatomy where there is not much intrinsic motion but where there may be induced physiological changes or induced changes brought about by the introduction of artificial contrast enhancement media such as gadolinium-DTPA.

An important aspect of high-speed imaging is the time spent in the machine by the patient. Current machines are slightly claustrophobic and it is important with uncooperative patients to get them out of the machine as soon as possible. This is especially true of young children where it is considered to be undesirable to use general anaesthetics or sedation. A consequence of the short examination procedure inherent with EPI is faster patient throughput. This aspect has important economic implications and ultimately will be the deciding factor in the widespread application of NMR imaging systems in the Health Service in Britain and in other countries. EPI is able to increase the patient throughput from typically one patient per hour in current commercial systems, to around four patients per hour with our prototype EPI scanner. Naturally, the imaging time depends very much on what is being studied, and clearly in some applications such as gut motility studies the imaging procedure, even with EPI, can take half an hour per patient by virtue of the fact that one is studying a relatively slow physiological process. The same is also true for gadolinium uptake studies. Nevertheless, there are many more applications which involve lesion detection where the imaging procedure is much more straightforward, and the total time that a patient needs to be in the machine can be as little as five minutes.

The basic principles of EPI based on the k-space approach will be described. Evolution of the technique to incorporate rapid spin lattice relaxation time and other NMR parameters will be briefly described and examples of these applications presented.

The first clinical applications of ultra-fast high-speed imaging will be based on single-slice and multislice use. However, it is possible to capture the data simultaneously from many slices in a single-shot process called echo-volumar imaging (EVI). This is technically more difficult and is therefore at an earlier phase of its evolution. Some description of this technique and the problems associated with it will be presented.

2. Method

In EPI methods (Chapman *et al.* 1987; Howseman *et al.* 1988; Turner *et al.* 1988; Stehling *et al.* 1989) a slice selection procedure (Garroway *et al.* 1974) produces signal from the active slice of material under examination. Following this process, the free induction decay (FID) is sampled for a time T in the presence of at least one

PHILOSOPHICAL TRANSACTIONS OF THE ROYAL SOCIETY A MATHEMATICAL, PHYSICAL & ENGINEERING SCIENCES

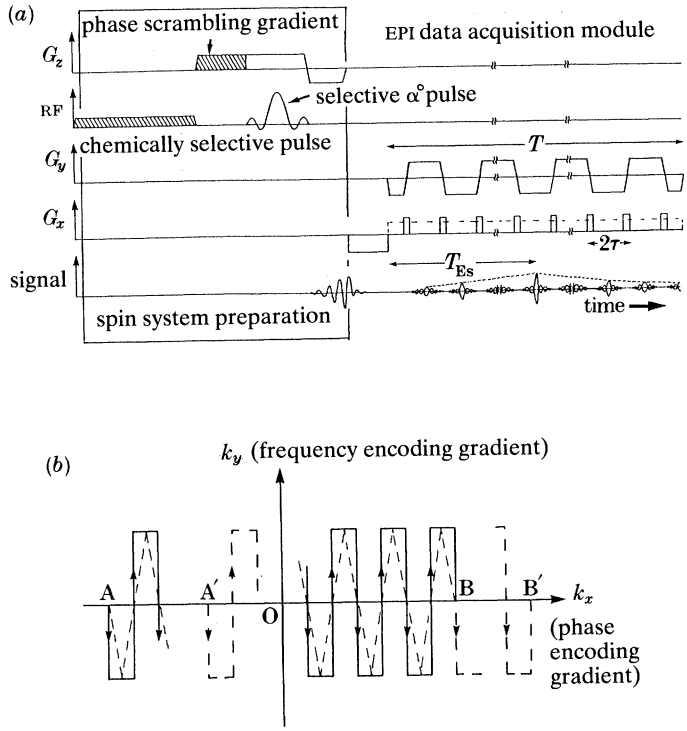

Figure 1. Diagram emphasizing the modular approach to EPI. (*a*) Pulse timing diagram showing gradient and RF details for the spin preparation phase followed by the EPI data acquisition module. The G_x gradient can take the form of a series of short blips or a constant low level gradient (dotted line). (*b*) k trajectory scan corresponding to EPI. The dotted zig-zag curve is the trajectory corresponding to the constant low level G_x gradient. For normal k-space scans ($T_{Es} = \frac{1}{2}T$) the scan starts at A and finishes at B. For shifted k-space scans the start occurs at A′ closer to the origin O and ends at B′.

trapezoidally or sinusoidally modulated gradient G_y (figure 1). The linear gradient G_y imposes a y coordinate axis on the excited slice with spatial discrimination along y. The bipolar modulation produces a set of spin echoes or gradient echoes. If a negative G_x prepulse is applied, the spin phase is preconditioned so that the fast echo train builds up to a maximum signal strength in a time T_{Es}, a slow echo time. The unwinding of the spin phase means that T_{Es} can occur early or at time $\frac{1}{2}T$ for correct spatial resolution. This is the procedure used in modulus EPI.

The x-axis encoding is achieved by application of a series of short pulse encoding blips (figure 1*b*) or a long continuous low-level gradient (dotted). In the k-space diagram (Mansfield & Grannell 1973, 1975; Ljunggren 1983) the trajectory is either a rectangular grid (blipped G_x) or a zig-zag path (dotted) corresponding to a continuously applied gradient. In either case the FID signal is sampled, reordered and Fourier transformed usually in a single 16 k fast Fourier transform (FFT) using an array processor (AP). For real-time applications the FFT must be less than 100 ms if repetition frame rates of 10 frames per second are to be achieved for real-time movie applications (Doyle *et al.* 1986; Chapman *et al.* 1987). In our home-built system, using an Analogic AP 500, the FFT for a 16 k array is achieved in 60 ms.

The total data acquisition time T is typically 64 ms for a 128×64 pixel array and 128 ms for a 128×128 pixel array. In the latter case, the receiver bandwidth is

± 128 kHz when linear signal sampling is used. More commonly, we use nonlinear sampling (Mansfield & Ordidge 1983) to compensate for the rise and fall times of our trapezoidally modulated waveforms. In this case a slightly higher bandwidth is required.

In the time T, the spin echo train signal can decay away due to T_2 and T_2^*. In the latter case a good magnet is required. Our homogeneity is ± 2 p.p.m. over a 30 cm diameter spherical volume, which at 0.5 T or 22 MHz for protons seems adequate for our purposes. For modulus EPI the origin of k-space occurs at T_{E_s}. Thus when $T_{Es} = \frac{1}{2}T$ we have a normal k-space origin, whereas shifted k-space scans occur when $T_{Es} < \frac{1}{2}T$ (typically $T_{Es} = \frac{1}{4}T$ or $\frac{1}{3}T$). The shortening of T_{Es} means that T_2 weighting can be varied. If $T_{Es} = 0$ this corresponds to an amplitude signal version of EPI with little T_2 weighting.

For rapid imaging at high frame rates, a low angle selective pulse (Mansfield 1984) is used to initially excite the magnetization slice. In some of the earlier amplitude EPI work a combination of low angle and 90° selective pulses were used in a snapshot method lasting *ca.* $2T$ (Chrispin *et al.* 1986). We refer to this as a two-pass method. The idea is readily extended to N passes for the generation of larger image arrays and higher spatial resolution (Mansfield & Ordidge 1983; Pykett & Rzedzian 1987).

3. Technical

Much of the initial scepticism to EPI was based on the fact that the method required much larger gradients, faster rise times, larger bandwidths and higher data rates than the then current commercial machines. There was also the vexed question of magnet stability and induced currents in the cryostat walls arising from the fast gradient switching.

In fact, with the passage of time, the capability of commercial machines has been steadily upgraded so that virtually all the special requirements are either currently available or are in the process of being made available. The eddy current problem has been solved by the introduction by Mansfield & Chapman in 1986 of the active magnetic screening of gradient coils (Mansfield & Chapman 1986*a*, *b*; 1987). The idea has been implemented on all GE machines and is being tried out by some other companies.

In fact, the special hardware requirements of other high-speed imaging methods like FLASH and snapshot FLASH are fast approaching those of EPI and indeed in some requirements they may actually exceed those of EPI.

4. Safety

The question of patient safety regarding induced currents due to fast magnetic field switching has always been of concern in EPI. Indeed there was much misplaced doomsaying about the use of switched gradients in the early days when the principles of slice selection were introduced (Garroway *et al.* 1974). Of course it is proper to have due regard to safety methods. In this respect the National Radiological Protection Board (NRPB) have issued guidelines on the acceptable limits for magnetic field switching rates in clinical MRI. Their current formula, which we work to, suggests that the rate of change of magnetic field $\mathrm{d}B/\mathrm{d}t$ should satisfy the condition $(\mathrm{d}B/\mathrm{d}t)^2 t < 4\ \mathrm{T}^2\ \mathrm{s}^{-1}$, where $\mathrm{d}B/\mathrm{d}t$ and the switching duration t are measured in units of teslas per second and seconds respectively.

PHILOSOPHICAL TRANSACTIONS OF THE ROYAL SOCIETY A MATHEMATICAL, PHYSICAL & ENGINEERING SCIENCES

For our EPI parameters, the maximum value $(\mathrm{d}B/\mathrm{d}t)_{\max} = 10\ \mathrm{T\ s^{-1}}$ and $t \approx 150\ \mu\mathrm{s}$ giving a product of $1.5 \times 10^{-2}\ \mathrm{T^2\ s^{-1}}$ which is well below the limits for induced neural stimulation. The NRPB guidelines are under review but it is not anticipated that EPI will exceed the new guidelines.

There is some growing evidence from other groups working with EPI (Cohen *et al.* 1990) that when $\mathrm{d}B/\mathrm{d}t \geqslant 80\ \mathrm{T\ s^{-1}}$, mild peripheral neural stimulation occurs. However, it should be noted that in some early unpublished work of ours on anaesthetized rats, attempts to interfere with the cardiac cycle using much higher values of $\mathrm{d}B/\mathrm{d}t$ in single pulses produced no effects whatsoever on the ECG. Thus it needs to be appreciated that even if peripheral neural stimulation or mild tingling is produced, although possibly uncomfortable it need not be dangerous.

The NRPB guidelines are under review and it seems likely that they will adopt the neural stimulation approach advocated by Mansfield & Morris (1982), in which a simple product formula $(\mathrm{d}B/\mathrm{d}t)\,t$ is used. However, since the neural stimulation model (Hodgkin 1967) depends on electrical charging of the nodal capacitance, a more appropriate approach is that based on accumulated charge. The charge q is proportional to

$$\exp(-t/\tau_{\mathrm{m}}) \int \exp(t'/\tau_{\mathrm{m}})\,(\mathrm{d}B/\mathrm{d}t')\,\mathrm{d}t',$$

where τ_{m} is the nodal membrane time constant. This means that for short times, i.e. $t/\tau_{\mathrm{m}} < 1$, the neural stimulation threshold is essentially independent of the rate of change of B and depends only on the total change ΔB. Full details of this work are described elsewhere (Mansfield 1991).

5. Susceptibility

EPI being a snapshot method has an intrinsically lower signal-to-noise ratio (SNR) than that obtained in slower imaging methods where data acquisition is spread over a longer time interval. Nevertheless, it is somewhat surprising to note that the signal-noise ratio difference need not be that large. For example if we compare SNR for a 128 ms EPI acquisition with that for a 128×128 array 5 ms window slow acquisition image, the improvement is only $\sqrt{5}$ if both images are obtained at the same field strength. Of course the EPI image may be compensated by a $\sqrt{5}$ increase in the magnetic field strength. However, field increase must be accompanied by a corresponding decrease in the magnetic field inhomogeneity. Higher fields also increase the problems of susceptibility mismatch, especially at the bone–tissue and tissue–gas interfaces. The effects can degrade EP images by introducing local field distributions and if particularly severe, by loss of signal due to local spin dephasing. These image artefacts can be mitigated to various extents by using larger spatial and phase encoding gradients so that local magnetic effects are swamped. This means reducing T and accepting a lower SNR. A better way is to use occasional short non-selective 180° RF pulses to effectively remove the induced static magnetic susceptibility effects. Of course, one could use all 180° RF pulses as an alternative to y-gradient modulation as suggested in the original papers on EPI (Mansfield 1977; Mansfield & Pykett 1978). However, that approach could produce an unacceptably higher RF power deposition in the patient, especially at high RF frequencies.

The large encoding gradients and short acquisition time of FLASH related imaging methods make these techniques intrinsically more robust to susceptibility effects.

Variants of EPI designed to measure chemical shift and its spatial distribution have been developed (Mansfield 1984; Guilfoyle & Mansfield 1985; Doyle & Mansfield

PHILOSOPHICAL TRANSACTIONS OF THE ROYAL SOCIETY A MATHEMATICAL, PHYSICAL & ENGINEERING SCIENCES

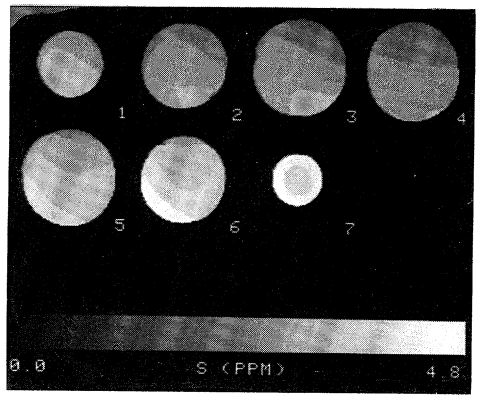

Figure 2. Magnetic field contours measured with PEEP imaging and corresponding to seven sections through a 22 cm diameter spherical water phantom. The contours are 0.3 p.p.m. apart. Slice separation is 20 mm.

1987; Guilfoyle *et al.* 1989; Bowtell *et al.* 1989), but have not yet been seriously exploited. By their nature they can be directly applied to the mapping of susceptibility. A particular method called phase-encoded echo-planar (PEEP) imaging (Guilfoyle *et al.* 1989) is able to map magnetic field inhomogeneity and susceptibility as well as produce distortionless images. It is not as fast as the echo-planar shift mapping (EPSM, pronounced epsem) method (Guilfoyle & Mansfield 1985), but is typically a factor 100 faster than three-dimensional FT methods.

An example of magnet homogeneity measurement using modulus PEEP is shown in figure 2. Here seven images of a 22 cm diameter spherical water phantom show the variations in magnet homogeneity by displaying bands of intensity within a particular image plane. The slice thickness is 10 mm and the slice separation is 20 mm. Each image comprises 64×64 pixels with a chemical shift axis δ of 128 points with 0.3 p.p.m. per point. In the central plane 4, for example, most of the image comprises two field contour bands giving a homogeneity of *ca.* 0.6 p.p.m. In the adjacent slice 3, the appearance of four bands indicates a chemical shift variation 1.2 p.p.m. Over the whole volume a total variation of 2.1 p.p.m. is indicated.

6. Preconditioning and the modular approach

Although EPI has evolved as a fast imaging technique for the study in medicine of normal morphology and the abnormal morphology associated with pathology and congenital defects, a growing use in our laboratory is that of prefixing the EPI sequence, treated as a read-out module, with a spin conditioning phase, figure 1*a*.

Spin conditioning can take several forms embracing the use of contrast media like Gd-DTPA (Mansfield *et al.* 1989) on the one hand to spin sensitization sequences to various NMR imaging parameters on the other. Spin conditioning comprises inversion recovery for T_1, spin echo sequences for T_2, chemical shift selectivity and flow and diffusion encoding. The NMR imaging parameters associated with all these effects can be mapped rapidly using EPI, thus making it an extremely versatile read-out module. In the case of flow, real-time flow only images are possible in which the image intensity at a particular point in the image is a function of the local fluid/object velocity (Guilfoyle *et al.* 1990).

PHILOSOPHICAL TRANSACTIONS OF THE ROYAL SOCIETY A MATHEMATICAL, PHYSICAL & ENGINEERING SCIENCES

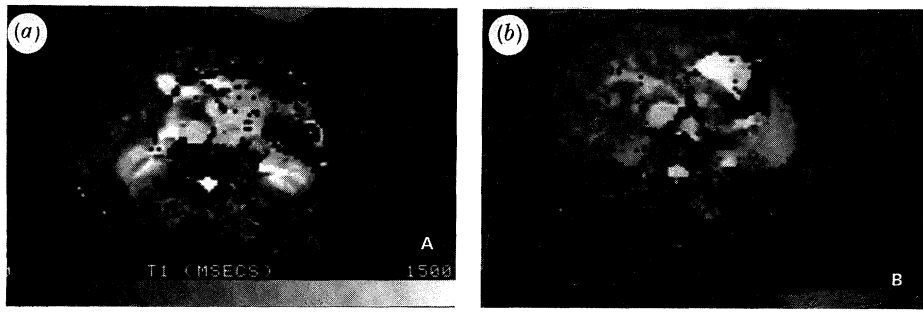

Figure 3. Spin lattice relaxation time (T_1) maps measured by an 8 time point fit using inversion-recovery EPI. (*a*) A scan through the kidneys. (*b*) Scan through the liver, stomach and spleen.

Figure 3 shows two examples of T_1 maps obtained from inversion-recovery EPI (Ordidge *et al.* 1990). These are from a rapid multi-slice set of eight T_1 maps all obtained in a total time of 30 s. Figure 2*a* corresponds to a 10 mm section through the kidneys of a normal volunteer. Figure 2*b* is 80 mm higher and depicts stomach, spleen and vascular detail in the liver.

7. Movement

One of the major attractions of EPI is its ability to image rapidly moving objects like the heart. It is true that with regular motion slower imaging methods can be gated with the ECG to build up the image or series of images over several hundred cardiac cycles. These can be subsequently played back to demonstrate movement. However, with ectopic beats or when the heart is in atrial fibrillation, gating methods are less valuable. EPI on the other hand can capture a complete movie at up to 10 frames per second (Doyle *et al.* 1986; Chapman *et al.* 1987) and is thus able to produce useful diagnostic images of the heart in otherwise difficult cases.

Figure 4 shows cardiac snapshot images of a normal heart taken during systole and diastole using a surface coil (Stehling *et al.* 1989). These images have an in-plane resolution of just under 2 mm and were obtained with an exposure or imaging time of 64 ms. They demonstrate clearly the changes in the myocardial wall thickness occurring during the heart cycle.

High-speed capability is especially useful when studying the human fetus *in utero* (Johnson *et al.* 1990; Mansfield *et al.* 1990; Stehling *et al.* 1990). Figure 5 shows a snapshot transection through a fetal abdomen (fa) in which a gastroschisis is evident. The prolapsed intestines (i) are seen floating in the amniotic fluid. The abdominal fissure is also seen. Part of a fetal limb (fl) and the placenta (p) are also depicted. The dark outline around the fetus corresponds to a subcutaneous fat layer. The fat signal is removed by selective pre-saturation. Some maternal structure is also evident including vertebra (mv) and spinal canal (msc).

8. Echo-volumar imaging (EVI)

Although EPI represents a great stride forward in nuclear magnetic resonance imaging, there are still problems when imaging a moving object in a single plane. This is particularly the case for the heart. During a cardiac cycle there is considerable movement in and out of the imaging plane which cannot be followed in a single plane

PHILOSOPHICAL TRANSACTIONS OF THE ROYAL SOCIETY A MATHEMATICAL, PHYSICAL & ENGINEERING SCIENCES

Figure 4

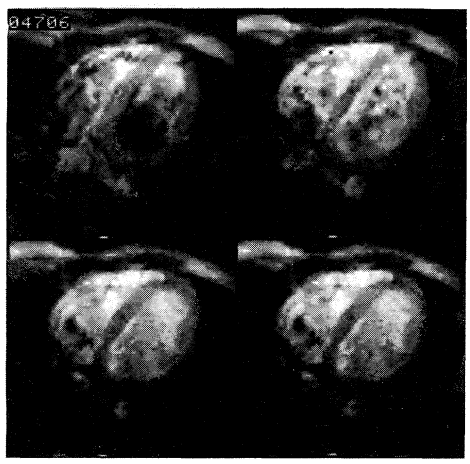

Figure 5

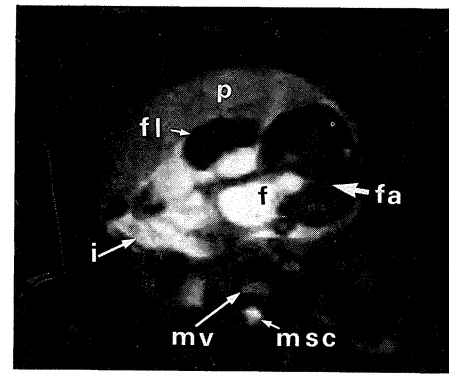

Figure 4. Four echo-planar snapshot images through the heart of a volunteer. A single surface coil was used to obtain these data. (*a*) and (*b*) show myocardial wall thickening of the left ventricle in systole. (*c*) and (*d*) correspond to slightly different phases in diastole and show corresponding thinning of the myocardium. The dark zones within the left ventricle correspond to rapid turbulence of the blood. Less turbulent and static blood show as bright signals. (Stehling *et al.* 1989.)

Figure 5. Snapshot image through a foetus *in utero* showing a gastroschisis. The foetal abdomen (fa) with fissure (f) is indicated together with intestines (i) floating in the amniotic fluid. The placenta (p) is also depicted together with part of a foetal limb (fl). The maternal vertebra is shown (mv) and the maternal spinal column (msc). This image was obtained in the 39th week of gestation.

movie. This third axis motion is exacerbated by respiratory motion. Multi-slice EPI does not help in this matter. It is in general difficult to match a series of contiguous planes through the mediastinum in a series of separate movies, an important point when looking for coronary vessels, the ultimate objective of much of current cardiac imaging research.

Echo-volumar imaging (Mansfield *et al.* 1989) overcomes the motional problems referred to above by arranging to receive data simultaneously from all regions of a predetermined volume that encompasses the object of interest. This is achieved by using an initial thick slice selection procedure followed by spatial and phase encoding along the three principal axes using suitably modulated magnetic field gradients, G_x, G_y and G_z. Various forms of EVI have been tried out including a four- and a two-pass version. But the method is only likely to be of value clinically in its true one shot form.

Figure 6 shows some early and rather crude four pass echo-volumar images of a water filled conical flask obtained at 0.1 T. The full data array comprises 1024 voxels formed into 16 planes each containing an 8×8 pixel array. The in-plane resolution was 24 mm and each plane thickness was 6 mm. Hardware improvements including higher field strength have allowed one shot whole-body EVI images to be produced with eight planes comprising 32×64 pixels (Harvey & Mansfield 1991).

The technical problems are greater and the hardware requirements are more stringent for EVI than for EPI. This is likely to limit the technique to images with relatively few pixels. However, if combined with zonal magnification or zooming (Mansfield *et al.* 1988) small total voxel arrays of say 64 k points could still be

PHILOSOPHICAL TRANSACTIONS OF THE ROYAL SOCIETY A MATHEMATICAL, PHYSICAL & ENGINEERING SCIENCES

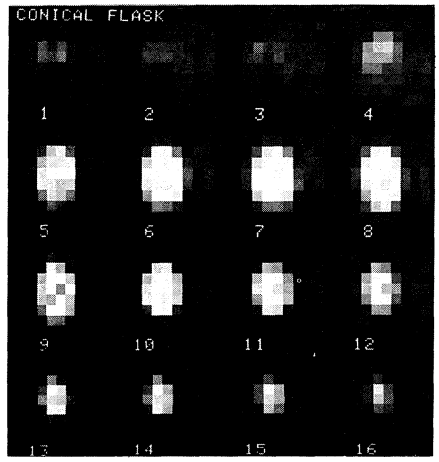

Figure 6. Echo-volumar images obtained from a water-filled conical flask phantom. The total imaging matrix consists of 1024 points represented here as 16 planes, each comprising an 8×8 pixel array. The base of the flask corresponds to images 4 and 5 and the scans proceed through the length of the flask tapering at the neck, images 15 and 16. The in-plane resolution is 24 mm and the selective slice thickness for all 16 planes was 90 mm. (Mansfield *et al.* 1989.)

clinically useful for imaging the heart. EVI arrays of this size with millimetre resolution have not yet been achieved but have come closer to practical realization by using a novel approach to the generation of square or trapezoidally shaped gradient waveforms based on multimode resonant gradient coils (Mansfield *et al.* 1991).

9. Conclusions

Much of the clinical MRI currently being done with slow commercial imaging machines could be performed with EPI in its present state of development. Of course, resolution and image quality in EPI can be improved and image arrays comprising 256×256 pixels are technically feasible with current technology. With higher magnetic field strength image quality can be increased and slice thickness reduced. Higher field strengths will also allow the proper development of echo-planar related spectroscopic imaging techniques.

The use of EPI as a spin state interrogation module has been emphasized with reference to T_1 mapping and flow. Other applications including diffusion will follow.

The major power of EPI is the ability to capture motion. In this regard it is valuable as a means of following the time course of a range of physiological functions including GI tract motility, CSF dynamics, cardiac function and dynamic uptake of contrast agents.

Perhaps the most recent exciting development in ultra-high-speed imaging is EVI. All the above comments regarding functional applications will apply to EVI. The difference is that EVI will not suffer from through plane object motion.

We thank the Medical Research Council and the Department of Health for major financial support of the echo-planar imaging programme. We also thank the British Heart Foundation for contributing to our data acquisition and processing equipment. A.M.B., P.G., P.H. and M.S. thank the Science and Engineering Research Council for research studentships.

PHILOSOPHICAL TRANSACTIONS OF THE ROYAL SOCIETY A MATHEMATICAL, PHYSICAL & ENGINEERING SCIENCES

References

Bowtell, R. W., Cawley, M. G., Mansfield, P. & Clague, A. D. H. 1989 Proton chemical-shift mapping using PREP. *J. magn. Reson.* **8**, 634–639.

Chapman, B., Turner, R., Ordidge, R. J., Doyle, M., Cawley, M. G., Coxon, R., Glover, P. & Mansfield, P. 1987 Real-time movie imaging from a single cardiac cycle by NMR. *Mag. Reson. Med.* **5**, 246–254.

Chrispin, A., Small, P., Rutter, M., Coupland, R. E., Doyle, M., Chapman, B., Coxon, R., Guilfoyle, D. N., Cawley, M. G. & Mansfield, P. 1986 Transectional echo planar imaging of the heart in cyanotic congenital heart disease. *Ped. Radiol.* **16**, 293–296.

Cohen, M. S., Weiskoff, R. M., Rzedzian, R. R. & Kantor, H. L. 1990 Sensory stimulation by time-varying magnetic fields. *Mag. Reson. Med.* **14**, 409–414.

Doyle, M. & Mansfield, P. 1987 Chemical shift imaging: a hybrid approach. *Mag. Reson. Med.* **5**, 255–261.

Doyle, M., Chapman, B., Turner, R., Ordidge, R. J., Coupland, R. E., Morris, G. K., Worthington, B. S. & Mansfield, P. 1986 Real-time cardiac imaging of adults at video frame rates by magnetic resonance imaging. *Lancet* **ii**, 682.

Frahm, J., Haase, A., Matthaei, D., Hanicke W. & Merbold, K.-D. 1986 FLASH Imaging: rapid NMR imaging using low flip-angle pulses. *J. magn. Reson.* **67**, 258–266.

Garroway, A. M., Grannell, P. K. & Mansfield, P. 1974 *J. Phys.* C **7**, L457.

Guilfoyle, D. N. & Mansfield, P. 1985 Chemical-Shift Imaging. *Mag. Reson. Med.* **2**, 479.

Guilfoyle, D. N., Chapman, B., Blamire, A. M., Ordidge, R. J. & Mansfield, P. 1989 PEEP – a rapid chemical shift imaging method. *Mag. Reson. Med.* **10**, 282–287.

Guilfoyle, D. N., Gibbs, P., Ordidge, R. J. & Mansfield, P. 1991 Real-time flow measurements using echo-planar imaging. *Mag. Reson. Med.* (In the press.)

Haase, A., Matthaei, D. & Norris, D. 1988 Snapshot FLASH NMR imaging. *Proc. 8th A. Meeting, Society of Magnetic Resonance in Medicine*, Amsterdam, vol. 1, p. 364.

Harvey, P. & Mansfield, P. 1991 Improvements in echo-volumar imaging. (In the press.)

Hodgkin, A. L. 1967 *The conduction of the nervous impulse*, p. 60. Liverpool University Press.

Howseman, A. M., Stehling, M. K., Chapman, B., Coxon, R., Turner, R., Ordidge, R. J., Cawley, M. G., Glover, P., Mansfield, P. & Coupland, R. E. 1988 Improvements in snapshot nuclear magnetic resonance imaging. *Br. J. Radiol.* **61**, 822–828.

Johnson, I. R., Stehling, M. K., Blamire, A. M., Coxon, R. J., Howseman, A. M., Chapman, B., Ordidge, R. J., Mansfield, P., Symonds, E. M., Worthington, D. B. & Coupland, R. E. 1990 Study of internal structure of the human fetus *in utero* by echo-planar MRI. *Am. J. Obstetrics Gynecology*.

Ljunggren, S. 1983 A simple graphical representation of Fourier based imaging methods. *J. magn. Reson.* **54**, 338–343.

Mansfield, P. 1977 Multi-planar image formation using NMR spin echoes. *J. Phys.* C **10**, L55–L58.

Mansfield, P. 1984 Spatial mapping of the chemical shift in NMR. *J. magn. Reson. Med.* **1**, 370–386.

Mansfield, P. 1988 Review article: imaging by nuclear magnetic resonance. *J. Phys.* E **21**, 18.

Mansfield, P. 1991 A model for neural stimulation. (In the press.)

Mansfield, P. & Chapman, B. 1986*a* Active magnetic screening of gradient coils in NMR imaging. *J. magn. Reson.* **66**, 573.

Mansfield, P. & Chapman, B. 1986*b* Active magnetic screening of coils for static and time-dependent magnetic field generation in NMR imaging. *J. Phys.* E **19**, 540.

Mansfield, P. & Chapman, B. 1987 Multi-shield active magnetic screening of coil structures in NMR. *J. magn. Reson.* **72**, 211–233.

Mansfield, P. & Grannell, P. K. 1973 NMR diffraction in solids? *J. Phys.* C **6**, L432–L426.

Mansfield, P. & Grannell, P. K. 1975 Diffraction and microscopy in solids and liquids by NMR. *Phys. Rev.* B **12**, 3618.

Mansfield, P., Harvey, P. & Coxon, R. 1991 Multi-mode resonant gradient coils. (In the press.)

Mansfield, P., Howseman, A. M. & Ordidge, R. J. 1989 Volumar imaging using NMR spin echoes: echo-volumar imaging (EVI) at 0.1 T. *J. Phys.* **22**, 324–330.

PHILOSOPHICAL TRANSACTIONS OF THE ROYAL SOCIETY A MATHEMATICAL, PHYSICAL & ENGINEERING SCIENCES

Mansfield, P. & Ordidge, R. J. 1983 British Patent GB2107469A.

Mansfield, P., Ordidge, R. J. & Coxon, R. 1988 Zonally magnified EPI in real-time by NMR. *J. Phys.* E **21**, 275–280.

Mansfield, P. & Morris, P. G. 1982 *Advances in magnetic resonance* (ed. J. S. Waugh), Suppl. no. 2, *NMR imaging in biomedicine*. New York: Academic Press.

Mansfield, P. & Pykett, I. L. 1978 Biological and medical imaging by NMR. *J. magn. Reson.* **29**, 355–373.

Mansfield, P., Stehling, M. K., Bullock, P., Firth, J. L., Blamire, A. M., Ordidge, R. J., Coxon, R. & Gibbs, P. 1989 Dynamic EPI of the brain using Gd-DTPA. *Proc. 6th Radiological Symposium, Graz, 12–14 October*, p. 78.

Mansfield, P., Stehling, M. K., Ordidge, R. J., Coxon, R., Chapman, B., Blamire, A. M., Gibbs, P., Johnson, I. R., Symonds, E. M., Worthington, B. S. & Coupland, R. E. 1990 Echo-planar imaging of the human fetus *in utero* at 0.5 T. *Br. J. Radiol.* (In the press.)

Ordidge, R. J., Gibbs, P., Chapman, B., Stehling, M. K. & Mansfield, P. 1990 High speed multi-slice T_1 mapping using inversion-recovery echo-planar imaging (IR-EPI). *Mag. Reson. Med.* (In the press.)

Pykett, I. L. & Rzedzian, R. R. 1987 Instant images of the body by magnetic resonance. *Mag. Reson. Med.* **5**, 563.

Stehling, M. K., Howseman, A. M., Ordidge, R. J., Chapman, B., Turner, R., Coxon, R. J., Glover, P., Mansfield, P. & Coupland, R. E. 1989 Whole-body echo-planar MR imaging at 0.5 T. *Radiology* **170**, 257.

Stehling, M. K., Mansfield, P., Ordidge, R. J., Coxon, R. J., Chapman, B., Blamire, A. M., Gibbs, P., Johnson, I. R., Symonds, E. M., Worthington, B. S. & Coupland, R. E. 1990 Echo-planar imaging of the human foetus *in utero*. *Mag. Reson. Med.* **13**, 314–318.

Turner, R., Chapman, B., Howseman, A. M., Ordidge, R. J., Coxon, R. J., Glover, P. & Mansfield, P. 1988 Snap-shot MRI at 0.1 T using double-screened gradients. *J. magn. Reson.* **80**, 248.

Discussion

J. C. Waterton (*ICI Pharmaceuticals, U.K.*). As scientists, we may be interested in making measurements from our images, rather than merely viewing them qualitatively. These techniques produce enormous amounts of data. Is it now the case that a major limitation will be the time (and cost) of skilled people interpreting and making measurements on these images?

P. Mansfield. The original bottleneck in imaging was the time to capture the data. Imaging times are now so fast that the data mass can present something of an embarrassment of riches. In a typical examination lasting 10 min over 500 images are produced, all of which must be examined by skilled people. The new bottleneck is therefore at the viewing and interpretation stage rather than the data gathering phase. The major challenge for the future is therefore one of data reduction and automatic interpretation via sophisticated software algorithms. If the bulk of the work can be done by computer, this will reduce the burden and cost of skilled personnel, leaving the radiologist or clinician to make the diagnosis from a number of computer aided options.

P. A. Bottomley (*GE Research and Development Center, U.S.A.*). Professor Mansfield's model for the threshold level of $\mathrm{d}B/\mathrm{d}t$ required for nerve stimulation suggests that the threshold depends only on ΔB, independent of the duration over which ΔB is applied. This does not appear to be consistent with empirical evidence from the literature showing that the threshold for stimulation of visual 'magneto-phosphene'

PHILOSOPHICAL TRANSACTIONS OF THE ROYAL SOCIETY A MATHEMATICAL, PHYSICAL & ENGINEERING SCIENCES

sensations in the brain varies dramatically with the duration or frequency of the applied dB/dt, increasing as the period of the dB/dt decreases. Could he clarify the conditions under which the model is expected to apply?

P. Mansfield. The nodal electrical parameters of a neurone dictate a time constant of about 150 μs. Waveform changes which occur on a timescale less than 150 μs would therefore be expected to have a correspondingly reduced effect on dB/dt. For very large dB/dt, as in RF waveforms, for example, there is no peripheral neural stimulation observed. This is, I believe, because of the effect I have described. Magneto-phosphene and other induced stimulation effects are all produced at lower frequencies where stimulation period may exceed the time constant.

A. N. Garroway (*Naval Research Laboratory, U.S.A.*). Professor Mansfield presented the simple Hodgkins RC model for a neural cell and made the point that for times short compared to the RC time constant, the system acts as an integrator and so the magnitude of the driving field B is important, rather than dB/dt. Is the simple model sufficiently relevant at these short times of the order of 100 μs?

P. Mansfield. The nodal time constant for the neural model is approximately 150 μs, depending on the values of nodal capacitance and resistance. I would, therefore, expect the analysis presented to hold for times less than 150 μs. But the shorter the time the closer is the approximation.

G. K. Radda (*University of Oxford, U.K.*). I understand that at the recent meeting of the European Society of Magnetic Resonance in Medicine some experimental results on the effect of gradient switching on peripheral nerve stimulation have been reported. Apparently the threshold at which pain is induced is measurable and should be taken into consideration. Has Professor Mansfield any comments?

P. Mansfield. The reported work on neural stimulation is all done at relatively low frequencies so far as I am aware. My point, however, is that at high frequencies or fast switching rates, the stimulating process actually becomes independent of the switching rate or waveform and dependent on the amplitude of the magnetic field change. This effect does not seem to have been discussed by others, perhaps because high enough frequencies were not reached. As stated previously in answer to an earlier question, the rate of change of field in an RF pulse is enormous but does not produce neural stimulation. Why is that so? It must be because of the effect I have described, namely that the nodal capacitance is effectively acting as an integrator.

PHILOSOPHICAL TRANSACTIONS OF THE ROYAL SOCIETY A MATHEMATICAL, PHYSICAL & ENGINEERING SCIENCES

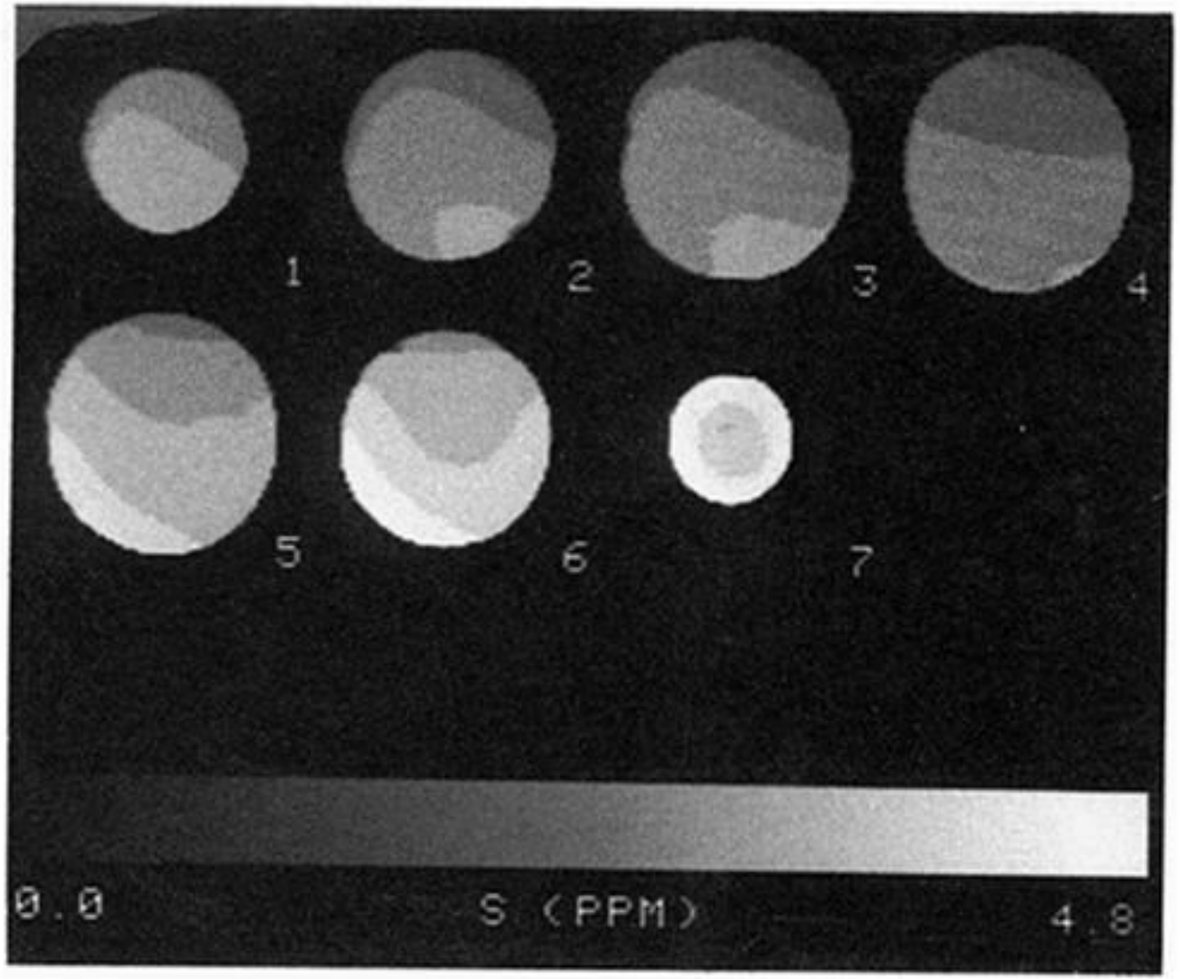

igure 2. Magnetic field contours measured with PEEP imaging and corresponding to seven sections rough a 22 cm diameter spherical water phantom. The contours are 0.3 p.p.m. apart. Slice paration is 20 mm.

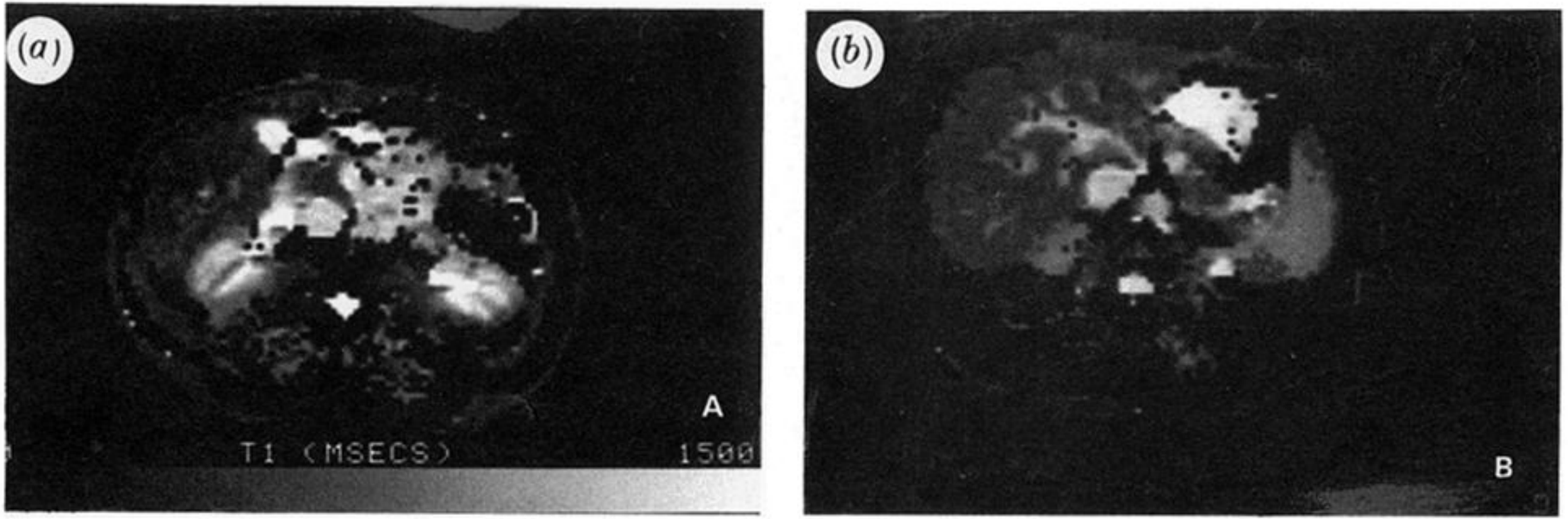

gure 3. Spin lattice relaxation time (T_1) maps measured by an 8 time point fit using inversion-ecovery EPI. (*a*) A scan through the kidneys. (*b*) Scan through the liver, stomach and spleen.

Figure 4

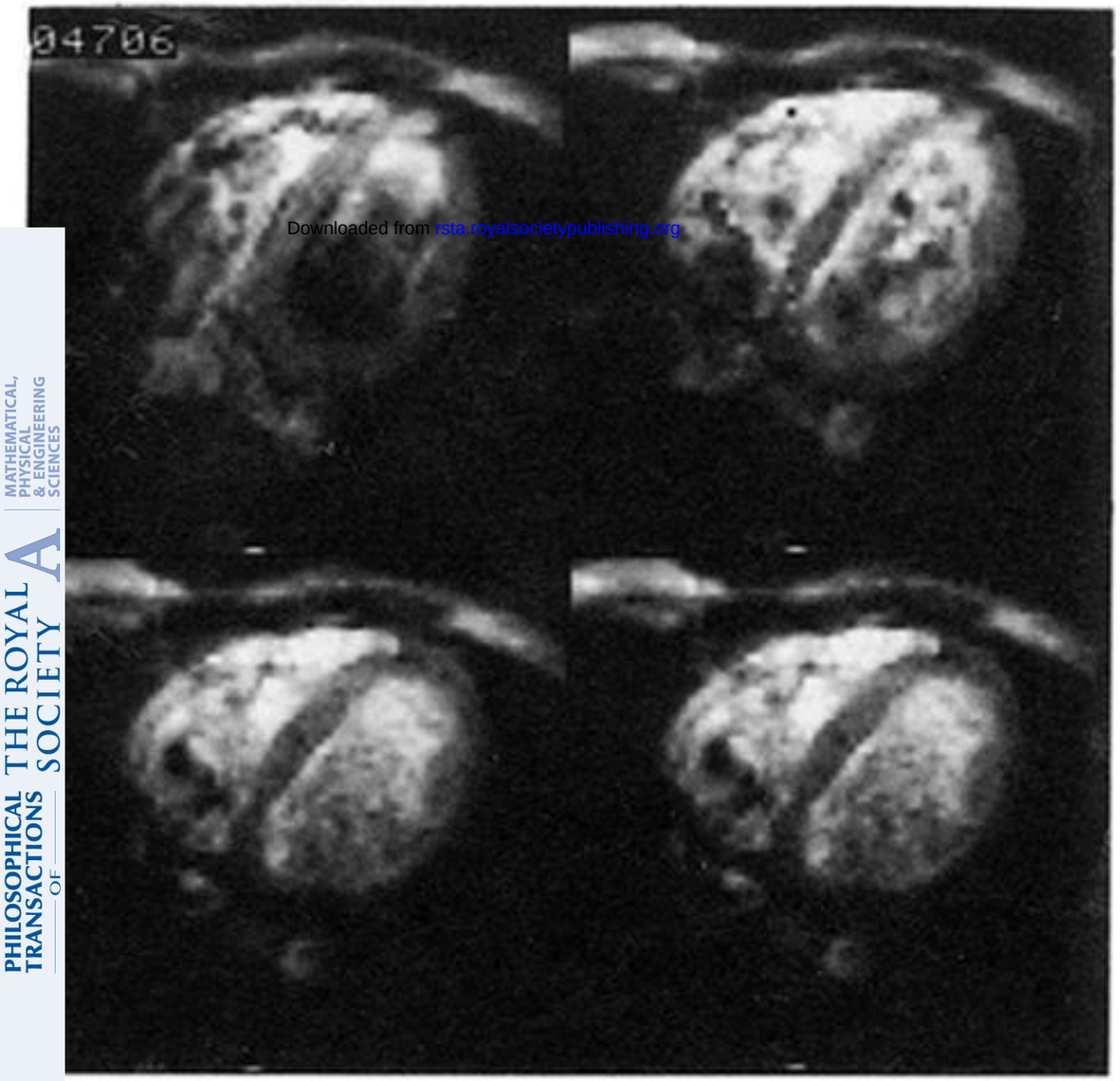

gure 4. Four echo-planar snapshot images through the heart of a volunteer. A single surface coil as used to obtain these data. (*a*) and (*b*) show myocardial wall thickening of the left ventricle in stole. (*c*) and (*d*) correspond to slightly different phases in diastole and show corresponding inning of the myocardium. The dark zones within the left ventricle correspond to rapid rbulence of the blood. Less turbulent and static blood show as bright signals. (Stehling *et al.* 89.)

Figure 5

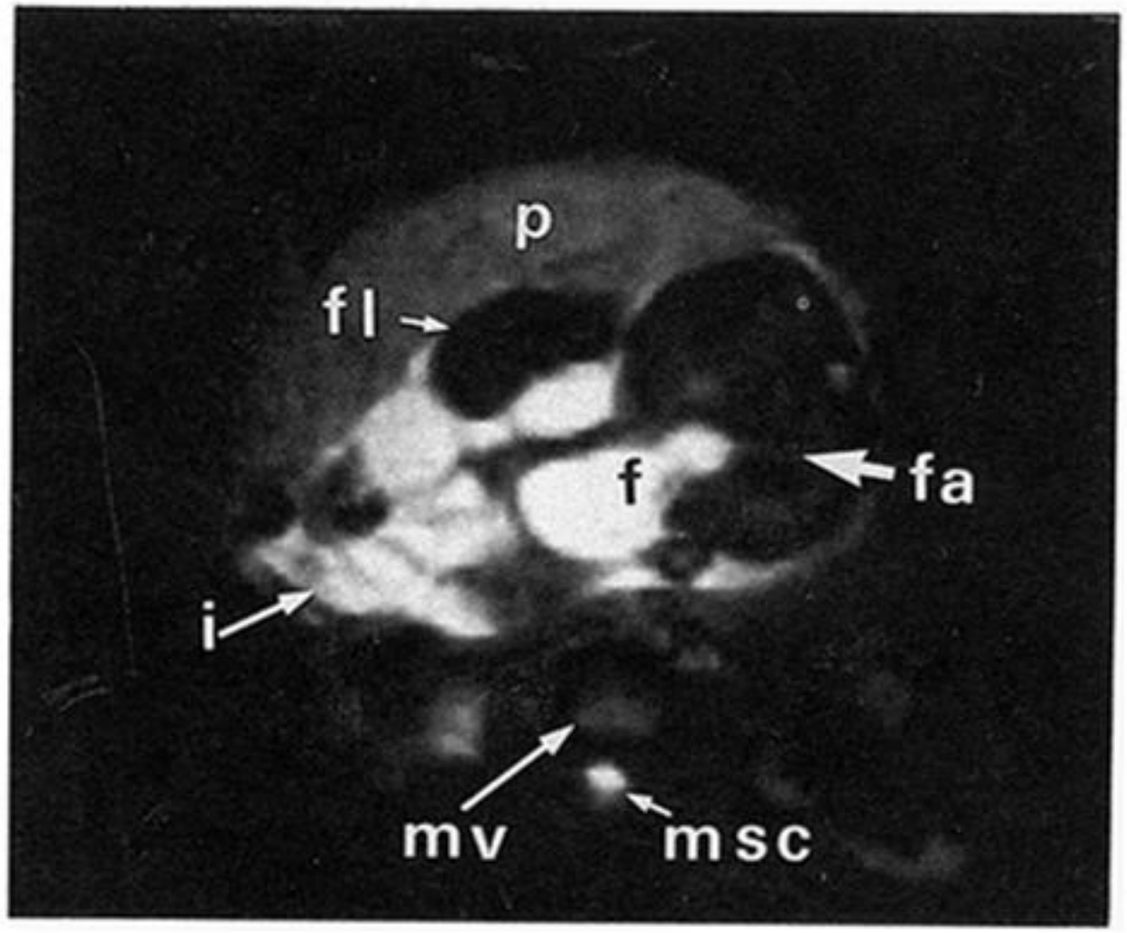

gure 5. Snapshot image through a foetus *in utero* showing a gastroschisis. The foetal abdomen (fa) th fissure (f) is indicated together with intestines (i) floating in the amniotic fluid. The placenta) is also depicted together with part of a foetal limb (fl). The maternal vertebra is shown (mv) and e maternal spinal column (msc). This image was obtained in the 39th week of gestation.

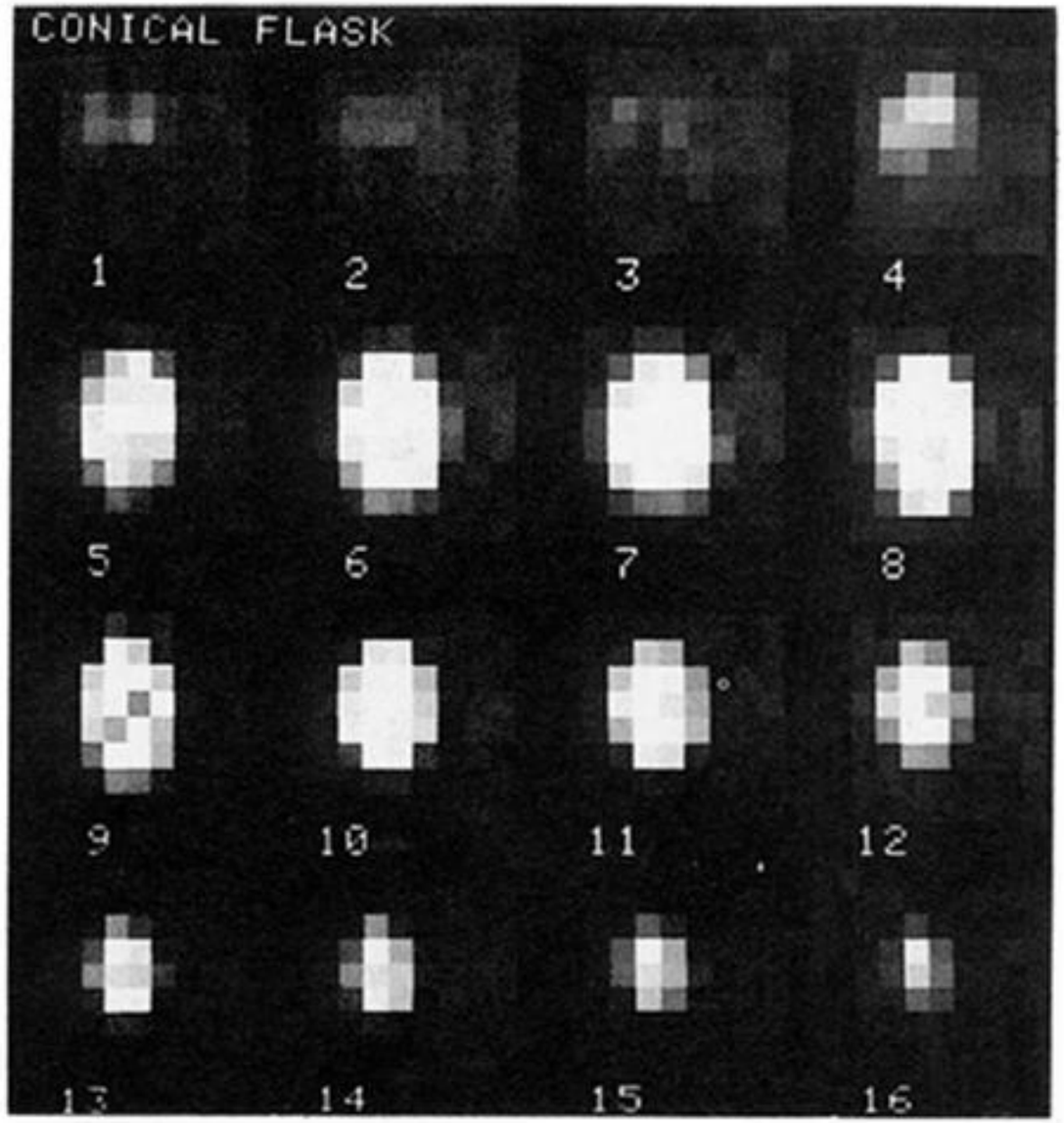

gure 6. Echo-volumar images obtained from a water-filled conical flask phantom. The total aging matrix consists of 1024 points represented here as 16 planes, each comprising an 8×8 pixel ray. The base of the flask corresponds to images 4 and 5 and the scans proceed through the length the flask tapering at the neck, images 15 and 16. The in-plane resolution is 24 mm and the lective slice thickness for all 16 planes was 90 mm. (Mansfield *et al.* 1989.)

PHILOSOPHICAL TRANSACTIONS OF THE ROYAL SOCIETY A MATHEMATICAL, PHYSICAL & ENGINEERING SCIENCES